

MOLECULAR OUTFLOWS IN GALAXY MERGER SIMULATIONS WITH EMBEDDED AGN

DESIKA NARAYANAN^{1,4}, THOMAS J. COX², BRANT ROBERTSON², ROMEEL DAVÉ¹, TIZIANA DI MATTEO³, LARS HERNQUIST², PHILIP HOPKINS², CRAIG KULESA¹, CHRISTOPHER K. WALKER¹

Accepted to The Astrophysical Journal Letters

ABSTRACT

We study the effects of feedback from active galactic nuclei (AGN) on emission from molecular gas in galaxy mergers by combining hydrodynamic simulations which include black holes with a three-dimensional, non-local thermodynamic equilibrium (LTE) radiative transfer code. We find that molecular clouds entrained in AGN winds produce an extended CO morphology with significant off-nuclear emission, which may be detectable via contour mapping. Furthermore, kinematic signatures of these molecular outflows are visible in emission line profiles when the outflow has a large line of sight velocity. Our results can help interpret current and upcoming observations of luminous infrared galaxies, as well as provide a detailed test of subresolution prescriptions for supermassive black hole growth in galaxy-scale hydrodynamic simulations.

Subject headings: cosmology: theory —galaxies: formation —active —interactions —ISM — line: formation

1. INTRODUCTION

The physical processes giving rise to the birth and sustained fueling of massive starbursts and active galactic nuclei (AGN) have been of interest since their discovery. It is generally agreed that AGN are powered by accretion of gas onto supermassive black holes (BHs) in the centers of galaxies (e.g. Lynden-Bell, 1969), but the fueling mechanism is less clear. Hydrodynamic simulations have shown that mergers can produce strong, galaxy-scale inflows owing to gravitational torques (Barnes & Hernquist 1991, 1996), triggering starbursts (Mihos & Hernquist, 1996). This suggests a circumstantial link between starbursts and AGN activity.

Observational evidence connecting the evolution of starbursts into AGN through mergers is compelling. Some ultraluminous infrared galaxies (ULIRGs, $L_{\text{IR}} \geq 10^{12} L_{\odot}$) exhibit spectral energy distributions (SEDs) characteristic of classical starbursts, whereas others have SEDs more closely resembling optical quasars (e.g. Farrah et al. 2003). In seminal papers, Soifer et al. (1987), and Sanders et al. (1988a,b) used optical, near infrared and millimeter-wave observations to advance a scenario in which starburst dominated ULIRGs served as antecedents of AGN. The specifics of a starburst-AGN connection, however, remain under heavy debate throughout the literature (e.g. Sanders & Mirabel, 1996).

Recent numerical models by Di Matteo, Springel & Hernquist (2005), Hopkins et al. (2005a-d), and Springel, Di Matteo & Hernquist (2005a) have provided a theoretical foundation for the link between starbursts and AGN. In particular, by modeling the growth of (and feedback from) central black holes, they showed that gas-rich galaxy mergers are a viable candidate to serve as a precursor to the formation of quasars. Their simulations also show that feedback from accreting black holes in galaxies are relevant to a wide range of phenomena associated with the evolution of galaxies in mergers including characteristic X-ray emission patterns (Cox et al. 2006), observed quasar luminosity functions and lifetimes

(Hopkins et al. 2005c), the $M_{\text{BH}} - \sigma$ relation (Di Matteo et al 2005; Robertson et al. 2006a), the fundamental plane of ellipticals (Robertson et al 2006b), and the bimodal galaxy color distribution (Springel, Di Matteo & Hernquist, 2005b; Hopkins et al. 2005e).

There has been a longstanding interest in better understanding the nature of the molecular interstellar medium (ISM) in mergers, as the molecular gas serves as fuel for the induced starburst activity and possibly for accreting BH(s). High resolution observations have identified massive concentrations of molecular gas in the nuclear regions of ULIRGs (Bryant & Scoville, 1999), as well as high excitation molecular gas in regions of massive starbursts (Iono et al. 2004; Wang et al. 2004).

Large surveys at submillimeter (sub-mm) and millimeter wavelengths have shown that mergers in the local Universe emit copious molecular line radiation both from diffuse molecular gas (e.g. Sanders, Scoville & Soifer, 1991, among others), and dense cloud cores (e.g. Gao & Solomon, 2004; Narayanan et al. 2005). Other work demonstrates that high- z infrared luminous and sub-mm selected sources also contain significant amounts of molecular gas (Greve et al. 2005; Tacconi et al. 2006). Moreover, as evidenced by IR and X-ray studies, a large fraction of these galaxies at high- z contain AGN (e.g. Alexander et al. 2005, Polletta et al. 2006). However, despite the wealth of data on molecular emission in interacting galaxies, little is known about the impact of embedded AGN on this radiation.

Here, we describe preliminary attempts to quantify the observable effects of AGN feedback on molecular line emission from major galaxy mergers. We use hydrodynamic simulations of mergers with and without AGN, combined with a new 3D non-LTE radiative transfer code (Narayanan et al. 2006a,b) to model CO emission. In this *Letter*, we describe results in which we find distinct signatures of AGN feedback on cold gas, and discuss some observational results that may be understood in this context.

2. NUMERICAL SIMULATIONS

Our hydrodynamic simulations were performed using the N -body/smoothed particle hydrodynamics (SPH) code, GADGET-2 (Springel, 2005). This code uses a fully conservative formulation of SPH (Springel & Hernquist 2002), and

¹ Steward Observatory, University of Arizona, 933 N Cherry Ave, Tucson, Az, 85721, USA

² Harvard-Smithsonian Center for Astrophysics, 60 Garden Street, Cambridge, MA 02138, USA

³ Carnegie Mellon University, Department of Physics, 5000 Forbes Ave., Pittsburgh, PA 15213

⁴ dnarayanan@as.arizona.edu

accounts for radiative cooling of the gas (Davé et al. 1999), a multi-phase description of the ISM which includes cold clouds in pressure equilibrium with hot, diffuse gas (e.g. McKee & Ostriker, 1977), and a prescription for star formation constrained by the Schmidt/Kennicutt laws (Kennicutt, 1998, Schmidt, 1959; see Springel & Hernquist, 2003). The black hole(s) in the simulation are realized through sink particles which accrete gas from the surrounding ISM such that 0.5% of the accreted mass energy onto the central black hole(s) is reinjected into the ISM as thermal energy (Di Matteo et al. 2005, Springel et al. 2005a,b).

The progenitor disk galaxies used in this work are similar to the Milky Way, but with a higher gas fraction (50%). Thus, they are likely representative of high- z disk galaxies, and possible progenitors of present epoch ULIRGs. The methodology for constructing the model galaxies is given in Springel et al. (2005a). The progenitors utilized a softened equation of state (EOS) with softening parameter $q_{\text{EOS}}=0.25$ (Springel et al. 2005a) such that the mass-weighted ISM temperature is $\sim 10^{4.5}$ K. The galaxies had dark matter halos initialized to follow a Hernquist (1990) profile, and circular velocity $V_{200}=160$ km s $^{-1}$. The virial properties of the halos are scaled to be appropriate for $z=2$ (e.g. Robertson et al. 2006a), and follow the prescription given by Mo et al. (1998) for cosmological models of disk galaxies. The galaxies were set on a parabolic orbit with the orientation of the spin axis of each disk specified by the standard spherical coordinates, θ and ϕ (with $\theta_1=30^\circ$, $\phi_1=60^\circ$, $\theta_2=30^\circ$, $\phi_2=45^\circ$), and were initially separated by 140 kpc. We utilize 120,000 dark matter particles, and 160,000 total disk particles, 50% of which represent gas, the rest serving as collisionless star particles. The gas, star, disk and dark matter particle masses were 3.9×10^5 , 1.95×10^5 , 5.9×10^5 and 7.6×10^6 $h^{-1}M_\odot$ each, respectively. The gravitational softening lengths were 100 h^{-1} pc for baryons, and 200 h^{-1} pc for dark matter particles. We have performed simulations with and without black holes. For the simulations with BHs, the initial mass of the BH particle in each progenitor 10^5 $h^{-1}M_\odot$, and the peak accretion rate was ~ 0.5 $M_\odot \text{yr}^{-1}$. The final mass of the remnant's BH is $\sim 5 \times 10^7$ $h^{-1}M_\odot$.

In order to estimate molecular line emission, we have developed a three dimensional non-local thermodynamic equilibrium (LTE) radiative transfer code based on an improved version of the Bernes (1979) algorithm. Our improvements (described more fully in Narayanan et al. 2006a,b) focus on including a subgrid model for giant molecular clouds (GMCs) in order to more accurately model the strongly density-dependent collisional excitation rates within our $\sim 10^2$ pc grid cells. We model GMCs as singular isothermal spheres (SISs) with power law index 2 (Walker, Adams & Lada, 1990), and assume half the cold gas mass in each cell is bound in GMCs. Our results for higher lying molecular levels and high dipole moment molecules are particularly improved using this sub-grid approach.

The emergent spectrum is built by integrating the equation of radiative transfer through numerous lines of sight. The source functions in each grid cell are determined by the densities of molecules at levels u and l for a given transition $u \rightarrow l$. These level populations, n_u, n_l are dependent on the incident radiation field from other clouds; we thus guess at a solution, calculate the mean intensity field in a Monte Carlo manner, determine the updated level populations through the rate equations, and repeat the process until the populations have converged. In between each iteration, the code goes into

a sub-resolution process in which it decomposes each cloud into a SIS and determines the level populations in each sub-resolution element. The non-LTE aspect of this treatment is particularly important as the assumption of LTE breaks down when considering the propagation of radiation through media with densities lower than the transition's critical density. For the radiative transfer calculations, we typically emitted $\sim 1 \times 10^7$ model photons per iteration, and consider the 2.73 K microwave background as the boundary condition.

3. RESULTS

3.1. Intensity Contour Maps

In Figure 1, we show a series of snapshots in CO ($J=1-0$) intensity contour maps from the two merger simulations. The plot spans 45 h^{-1} Myr, and begins when the progenitors are approaching final coalescence. The black hole accretion rate nears its peak as the black holes merge at $T \sim 1.15$ h^{-1} Gyr, and thus the feedback energy input from the AGN is near its maximum in the model with BHs.

Beginning from $T \approx 1.13$ h^{-1} Gyr onward, the CO morphology of the galaxy in the BH model undergoes dramatic changes owing to feedback from the buried AGN. Massive blobs of cold molecular gas entrained in the wind are visible through the CO ($J=1-0$) tracer. Indeed, while the AGN wind may in detail evaporate cold clouds via thermal conduction, enough cold gas survives to be visible through molecular emission. Moreover, the clouds entrained in these outflows remain cold and dense enough to continue forming stars. The dense cores in these clouds emit at CO transitions with relatively high critical densities; consequently, the outflows are visible against the background at transitions as high as CO ($J=6-5$). In order to produce the observed emission comparable to that of the nucleus, the outflows must have large column densities. We find columns ranging from $5 \times 10^{22} \text{cm}^{-2} \lesssim N(\text{H}_2) \lesssim 1 \times 10^{23} \text{cm}^{-2}$ through the outflow in Figure 1, depending on the viewing angle (although, we did not include a UV background in our models, and thus the true column may be less). As the outflowing gas leaves the nuclear region at velocities of ~ 200 -300 km s $^{-1}$, it becomes more diffuse, resulting in weaker CO emission. We find that the existence of molecular outflows is not unique to this particular model, and is seen in other merger simulations which include BHs.

In the model without BHs (right column, Figure 1), the molecular outflows on the \sim kpc scale observed in the BH model are not seen, highlighting the effects of AGN feedback in expelling loosely bound circumnuclear molecular gas. We note, however, that supernovae-driven winds are not incorporated in these models. It is known, through absorption line spectroscopy, that such winds in starbursts can induce outflows of comparable speeds (e.g. Heckman et al. 2000; Martin, 2005; Rupke et al. 2005). While large columns of outflowing molecular gas have not been imaged in many of these systems, there are notable exceptions such as the classic starburst M82 (Walter, Weiß & Scoville, 2002). We will explore the effects of supernovae winds on the molecular gas in due course.

3.2. Line Profiles

The AGN induced outflows also leave their imprint on spectral line profiles. In Figure 2, we have calculated the spectral line emission from $T = 1.155$ h^{-1} Gyr in the model with black holes (lower left panel in Figure 1). The spectrum is generated along three orthogonal lines of sight. In order to

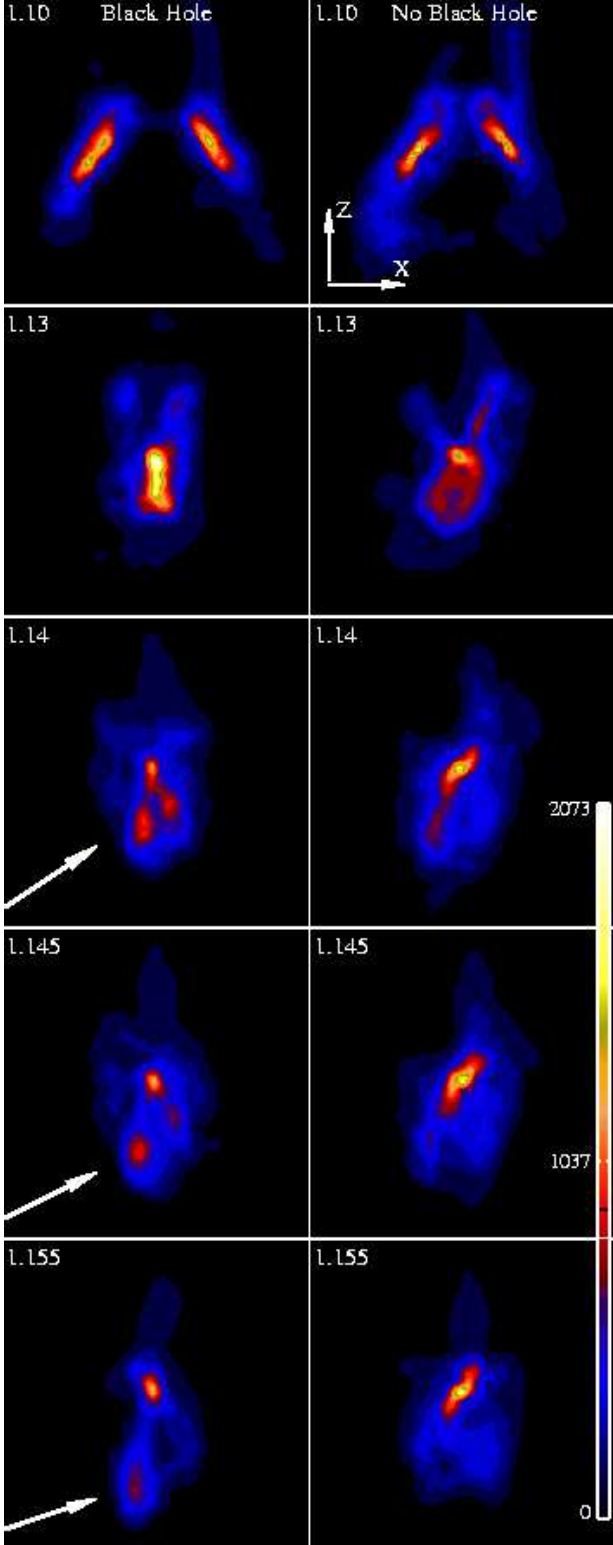


FIG. 1.— CO (J=1-0) emission intensity contours for an equal mass galaxy merger. The left column is a time sequence for the model with BHs, and the right column without BHs. In the model with BHs, after the galaxies merge, massive amounts of gas are driven into the nuclear regions and accrete onto the supermassive black hole. The subsequent AGN feedback energy can blow large blobs of molecular gas out from the nuclear regions (see arrows). These features are not seen in the model without BHs. The time stamp of the image is in the top left of each panel, and is in units of h^{-1}Gyr . The color contours are in units of K-km s^{-1} (velocity-integrated Rayleigh-Jeans temperature), and the scale is on the right side of the plot. Each panel is $12 \text{ h}^{-1}\text{kpc}$ on a side. The images are made at $1/4 \text{ h}^{-1}\text{kpc}$ spatial resolution. The coordinate system for use with Figure 2 is in the top right panel.

simulate an unresolved observation, we set the merger at $z=2$ ($\Omega_{\Lambda}=0.7$, $\Omega_M=0.3$, $h=0.75$), and convolved the emission from the $12 \text{ h}^{-1}\text{kpc}$ image with a circular $30''$ ($\sim 235 \text{ kpc}$) Gaussian beam.

Typically, in the BH model, once the galaxies have coalesced (when the BHs of the progenitors are indistinguishable in our simulations), the emission from the unresolved object is characteristic of a single Gaussian, centered at the systemic velocity of the galaxy. However, when viewing outflows with a strong line of sight (LOS) velocity component, a secondary peak appears superposed on the Gaussian emission line from the galaxy (e.g. left panel, Figure 2); this peak is the emission from the outflow, and is redshifted or blueshifted from line center at the LOS velocity of the outflow. While we have presented the CO (J=1-0) emission, these line profiles are similar through CO (J=6-5).

The emission peak corresponding to the outflow appears at the greatest offset velocity with respect to the systemic velocity of the galaxy when the outflow is moving mostly along the LOS (e.g. the $-\hat{z}$ observation, Figure 2). If the observation is tilted such that a smaller component of the outflow velocity is along the LOS, the emission peak corresponding to the outflow will move closer to, and eventually will merge with the broad emission peak of the galaxy (\hat{y} observation and $-\hat{x}$ observation, Figure 2, respectively). The peak temperature of the outflow emission may also decrease when the observation is tilted as the observer looks through less column. A given outflow along a particular line of sight is typically visible via its line profile for an average of $\sim 10 \text{ h}^{-1}\text{Myr}$ before the column density through the outflow drops such that its emission is no longer detectable against the broader Gaussian emission from the central region. We estimate the “outflow” profiles are visible $\sim 25\%$ of the time in our simulations (which span $200 \text{ h}^{-1}\text{Myr}$), averaged over many viewing angles.

Double-peaked profiles have been observed in mergers which do not necessarily correspond to outflows: for example, observations of high density gas in the prototypical ULIRG, Arp 220, have evidenced a symmetric double-peak profile where each peak corresponds to the starburst regions of nuclei of the progenitor galaxies (Taniguchi & Shioya, 1998, Sakamoto et al. 1999, Narayanan et al. 2005). Similar profiles also occur in systems in which there is significant rotation, i.e. a disk galaxy or rotating nuclear ring. However, some differences exist between the double peaks originating in progenitor galaxies or rotating systems, and those caused by outflows. The double peaks characteristic of the former two cases are typically both broad, and symmetric about the systemic velocity of the galaxy. Conversely, the peak arising from the outflow is typically much narrower than the broad emission profile of the galaxy, due to its small velocity dispersion along the LOS. That said, the component of the profile from the outflow can be quite bright, owing to large H_2 column densities through the outflowing material.

The characteristic outflow profile consisting of a broad Gaussian with a narrow line superposed is also degenerate with that of high velocity gas falling in toward the nucleus. The infalling clouds tend to have a higher velocity dispersion than clouds entrained in the AGN wind by, on average, $\sim 30\%$, resulting in broader CO lines. It is unclear, though, from our simulations whether there is a significant enough difference between the velocity dispersion or column density in outflowing and infalling gas to determine the direction of flow from CO observations alone. There may be observational tests at other wavelengths to help break this degeneracy, how-

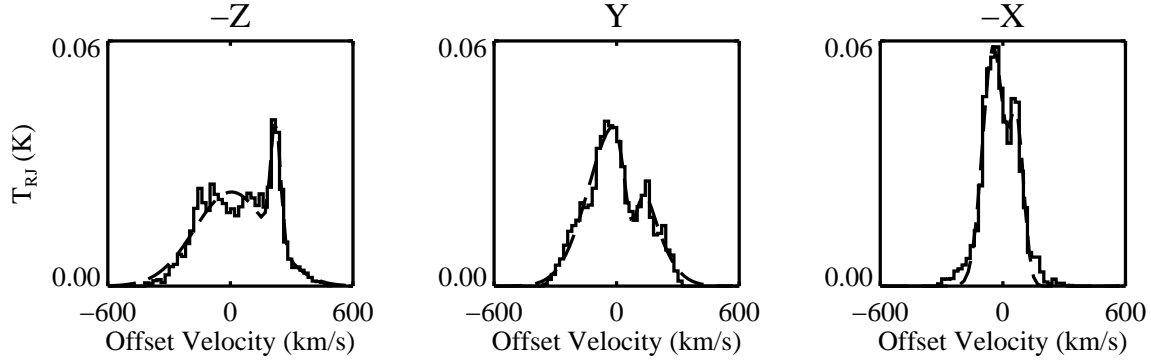


FIG. 2.— Synthetic CO ($J=1-0$) (rest-frame) emission line profile taken at $T=1.155 \text{ h}^{-1} \text{ Gyr}$ in the merger run with black holes over 3 orthogonal viewing angles. The direction of each line of sight is above the panels, and corresponds with the coordinate system in the top right panel of Figure 1. The high velocity peak in the leftmost panel owes to the outflowing gas viewed with a large line of sight velocity component. In the \hat{y} direction, the outflow has a smaller LOS velocity, and the emission owing to the outflow blends more into the main emission. In the $-\hat{x}$ viewing angle, outflows have a negligible effect on emission line. The best fit to the model spectra are overplotted with dashed lines. The spectra is taken such that the object is at $z=2$, and convolved with a $30''$ circular Gaussian beam.

ever. In our simulations, infalling gas primarily leaves its imprint on the line profile just as the major merger has occurred, prior to the major AGN feedback phase. By serving as an indicator for AGN activity, X-ray observations may help distinguish the origin of the “outflow” line profile. For example, using similar simulations to those explored in this study, Cox et al. (2006) have shown that the X-ray luminosity from diffuse gas in galaxy mergers peaks during the phase of heavy black hole accretion, and that thermal energy input from AGN feedback can produce X-rays consistent with observations of ULIRGs with known embedded AGN (e.g. UGC 5101, Imanishi et al. 2003). Elevated X-ray emission, both from diffuse gas, as well as hard X-rays from the central black holes may be indicative of a buried AGN. Correlations between hard X-ray flux and CO line profiles will be discussed in greater detail in Narayanan et al. (2006b).

At $z \approx 2$, where the infrared and submillimeter background are dominated by LIRGs and ULIRGs (Smail, Ivison & Blain, 1997), and the quasar density is near its peak (e.g. Schneider et al. 2005), large molecular line surveys may prove fruitful in investigating the existence of a correspondence between double-peaked line profiles and quasar activity. Indeed, large fractions of sub-mm galaxies at high redshift show double-peaked line profiles ($\sim 50\%$, Greve et al. 2005, Tacconi et al. 2006), some of which appear to have line profiles similar to those presented in the leftmost and middle panels of Figure 2; similarly, large fractions ($\sim 75\%$) of sub-mm galaxies show AGN activity as evidenced by IR and X-ray studies (Alexan-

der et al. 2005, Polletta et al. 2006).

4. SUMMARY AND CONCLUSIONS

We have discussed two features of CO emission from cold molecular gas entrained in winds resulting from AGN feedback in galaxy mergers: 1.) an extended CO morphology when the outflow is largely in the plane of the observation, and 2.) kinematic features in the emission line profile when the outflow has a significant line of sight velocity component. There may, of course, be hybrid cases as well, in which features of both signatures of AGN feedback are detectable.

Observations of signatures such as these can help to interpret current observations of ULIRGs both at low and high- z . Emission maps and line profiles similar to those presented in this work may have already been observed in local mergers (e.g. NGC 985, Appleton et al. 2001), as well as in $z \approx 2$ sub-mm selected sources (Greve et al. 2005, Tacconi et al. 2006). Upcoming surveys with high resolution interferometers have the potential of constraining models of black hole growth and associated AGN feedback in galaxy mergers.

D.N. acknowledges financial support from an NSF Graduate Research Fellowship, and thanks Brandon Kelly and Casey Papovich for helpful conversations. The calculations were performed on Grendel, a Steward Observatory Beowulf system.

REFERENCES

- Alexander, D.M., Smail, I., Bauer, F.E., Chapman, S.C., Blain, A.W., Brandt, W.N., Ivison, R.J., 2005, *Nature*, 434,730
 Appleton, P., Charmandaris, V., Gao, Y., Combes, F., Ghigo, F., Horellou, C., Mirabel, I.F., 2002, *ApJ*, 566,682
 Barnes, J.E., Hernquist, L.E., 1991, *ApJ*, 370, L65
 Barnes, J.E., Hernquist, L.E., 1996, *ApJ*, 471, 115
 Bernes, C., 1979, *A&A*, 73,67
 Bryant, P.M. & Scoville, N.Z. 1999, *AJ*, 117, 2632
 Cox, T.J., Di Matteo, T., Hernquist, L., Hopkins, P., Robertson, B., Springel, V., 2006, *ApJ*, in press [astro-ph/0504156]
 Davé, R., Hernquist, L., Katz, N., Weinberg, D.H., 1999, *ApJ*, 511,521
 Di Matteo, T., Springel, V., Hernquist, L., 2005, *Nature*, 433,604
 Farrah, D., Afonso, J., Efstathiou, A., Rowan-Robinson, M., Fox, M., Clements, D., 2003, *MNRAS*, 343,585
 Gao, Y., Solomon, P.M., 2004, *ApJ*, 606,271
 Greve, T.R. et al., 2005, *MNRAS*, 359,1165
 Heckman, T.M., Lehnert, M.D., Strickland, D.K., & Armus, L., 2000, *ApJS*, 129,493
 Hernquist, L., 1990, *ApJ*, 356,359
 Hopkins, P.F., Hernquist, L., Cox, T.J., Di Matteo, T., Martini, P., Robertson, B., Springel, V., 2005a, *ApJ*, 630, 705
 Hopkins, P.F., Hernquist, L., Martini, P., Cox, T.J., Robertson, B., Di Matteo, T., Springel, V., 2005b, *ApJ*, 625,L71
 Hopkins, P.F., Hernquist, L., Cox, T.J., Di Matteo, T., Robertson, B., Springel, V., 2005c, *ApJ*, 630, 716
 Hopkins, P.F., Hernquist, L., Cox, T.J., Di Matteo, T., Robertson, B., Springel, V., 2005d, *ApJ*, in press [astro-ph/0506398]
 Hopkins, P.F., Hernquist, L., Cox, T.J., Robertson, B., Springel, V., 2005e, *ApJ*, in press [astro-ph/0508167]
 Imanishi, M., Terashima, Y., Anabuki, N., Nakagawa, T., 2003, *ApJ*, 596, L167
 Iono, D., Ho, P.T.P., Yun, M.S., Matsushita, S., Peck, A., Sakamoto, K., 2004, *ApJ*, 616, L63
 Kennicutt, R., 1998, *ApJ*, 498,541
 Lynden-Bell, D., 1969, *Nature*, 223, 690
 Martin, C.L., 2005, *ApJ*, 621,227
 McKee, C.F., Ostriker, J.P., 1977, *ApJ*, 218,148
 Mihos, J.C., Hernquist, L.E., 1996, *ApJ*, 464,641

- Mo, H.J., Mao, S., White, S.D.M., 1998, MNRAS, 295,319
- Narayanan, D., Groppi, C.E., Kulesa, C.A., Walker, C.K., 2005, ApJ, 630,269
- Narayanan, D., Kulesa, C.A., Boss, A.P., Walker, C.K., 2006a, ApJ, in press
- Narayanan, D., Cox, T.J., Robertson, B., Davé, R., Di Matteo, T., Kulesa, C., Hernquist, L., Hopkins, P., Martini, P., Springel, V., Walker, C.K., 2006b, in preparation
- Polletta M., et al. 2006, ApJ, 642, in press [astro-ph/0602228]
- Robertson, B., Hernquist, L., Cox, T.J., Di Matteo, T., Hopkins, P.F., Martini, P., Springel, V., 2006a, ApJ, in press [astro-ph/0506038]
- Robertson, B., Cox, T.J., Hernquist, L., Franx, Marijn, Hopkins, P., Martini, P., Springel, V., 2006b, ApJ, in press [astro-ph/0511053]
- Rupke, D., Veilleux, S., Sanders, D.B., 2005a, ApJS, 160,87
- Sakamoto, K., Scoville, N.Z., Yun, M., Crosas, M., Genzel, R., Tacconi, L.J., 1999, ApJ, 514,68
- Sanders, D.B., Soifer, B.T., Elias, J.H., Madore, B.F., Matthews, K., Neugebauer, G., Scoville, N.Z., 1988a, ApJ, 325,74
- Sanders, D.B., Soifer, B.T., Elias, J.H., Madore, B.F., Matthews, I., Neugebauer, G., Scoville, N.Z., 1988b, ApJ, 325, 74S
- Sanders, D.B., Scoville, N.Z., Soifer, B.T., 1991, ApJ, 370,158
- Sanders, D.B., Mirabel, I.F., 1996, ARA&A, 34,749
- Schmidt, M., 1959, ApJ, 129,243
- Schneider, D.P. et al. 2005, AJ, 130,367
- Smail, I., Ivison, R.J., Blain, A.W., 1997, ApJ, 490, L5S
- Soifer, B.T., et al. 1987, ApJ, 320,238
- Solomon, P.M., vanden Bout, P.A., 2005, ARA&A, 43,677
- Springel, V., Hernquist, L., 2002, MNRAS, 333, 649
- Springel, V., Hernquist, L., 2003, MNRAS, 339, 312
- Springel, V., 2005, MNRAS, 364,1105
- Springel, V., Di Matteo, T., Hernquist, L., 2005a, MNRAS, 361,776
- Springel, V., Di Matteo, T., Hernquist, L., 2005b, ApJ, 620,L79
- Tacconi, L.J., 2006, ApJ, in press [astro-ph/0511319]
- Taniguchi, Y., Shioya, Y., 1998, ApJ, 501,L167
- Walter, F., Weiß, A., Scoville, N., 2002, ApJ, L21-L25
- Wang, J., Zhang, Q., Wang, Z., Ho, P.T.P., Fazio, G., Wu, Y., 2004, ApJ, 616, L67
- Walker, C.K., Adams, F.C., Lada, C.J., 1990, ApJ, 349,515